DOI: 10.1002/chem.200903336

VIP

Organosilyl/-germyl Polyoxotungstate Hybrids for Covalent Grafting onto Silicon Surfaces: Towards Molecular Memories

Nicoleta Joo,[a] Séverine Renaudineau,[b] Guillaume Delapierre,[a] Gérard Bidan,*[c] Lise-Marie Chamoreau,[b] René Thouvenot,*[b] Pierre Gouzerh,[b] and Anna Proust*[b, d]

Abstract: Organosilyl/-germyl polyoxotungstate hybrids $[PW_9O_{34}(t\text{BuSiO})_3Ge(CH_2)_2CO_2H]^{3-}$ (**1a**), $[PW_9O_{34}(t\text{BuSiO})_3Ge(CH_2)_2CONHCH_2C{\equiv}CH]^{3-}$ (**2a**), $[PW_{11}O_{39}Ge(CH_2)_2CO_2H]^{4-}$ (**3a**), and $[PW_{11}O_{39}Ge(CH_2)_2CONHCH_2C{\equiv}CH]^{4-}$ (**4a**) have been prepared as tetrabutylammonium salts and characterized in solution by multinuclear NMR spectroscopy. The crystal structure of $(NBu_4)_3$**1a**$\cdot H_2O$ has been determined and the electrochemical behavior of **1a** and **2a** has been investigated by cyclic voltammetry. Covalent grafting of **2a** onto an n-type silicon wafer has been achieved and the electrochemical behavior of the grafted clusters has been investigated. This represents the first example of covalent grafting of Keggin-type clusters onto a Si surface and a step towards the realization of POM-based multilevel memory devices.

Keywords: molecular memories · NMR spectroscopy · organic–inorganic hybrid composites · polyoxometalates · silicon · surface chemistry

Introduction

Polyoxometalates (POMs) are molecular nanosized transition-metal oxide clusters with a large variety of structures, properties, and applications in fundamental and applied science.[1] One of their most significant properties is the ability of type-I POMs according to Pope classification[2] to accept and release specific numbers of electrons with minimal structural change,[1–4] which makes them attractive candidates for the catalysis of redox reactions.[4–7] As soluble analogues of transition-metal oxides, POMs are also promising components for the design of advanced materials and functional devices.[8–9] Indeed POM-based hybrid materials have the potential for applications in sensors,[10–12] electro- and photochromic devices,[13,14] fuel cells,[15] photovoltaic cells,[16] energy storage,[17] and molecular electronics.[18] An attractive perspective is the realization of multilevel molecular memories based on semiconducting nanowire field effect transistors[19] or hybrid molecular-silicon capacitors[20] by using POMs as redox-active components.[21] The feasibility of such a project is supported by recent results from the groups of Glezos[18a,22] and Tour[23] on electron transport or charge confinement in POM-based molecular devices.

Applications of POMs usually require their immobilization onto an appropriate support or into an appropriate matrix. With regard to attachment of POMs onto electrodes, various methods can be used, for example, 1) spontaneous adsorption on electrode surfaces,[5,24,25] 2) electrodeposition under constant potential,[5] 3) entrapment in polymeric matrices,[25–30] and 4) layer-by-layer self-assembly of alternating layers of POMs and positively charged species.[7,31] The latter technique is especially attractive as it provides control of the structure of POM-based films at the nanometer scale. While most POM-based hybrid materials reported to date involve noncovalent interactions, for example, van der Waals contacts, hydrogen bonding, and ionic interactions, a few hybrid polymers involve covalent linking.[16,30a,32–35] Covalent grafting of POMs on surfaces is even more rare (vide

[a] N. Joo, Dr. G. Delapierre
CEA-LETI-DTBS Minatec, 17 rue des Martyrs
38054 Grenoble Cedex 9 (France)

[b] S. Renaudineau, L.-M. Chamoreau, Dr. R. Thouvenot, Prof. Dr. P. Gouzerh, Prof. Dr. A. Proust
Institut Parisien de Chimie Moléculaire
UMR CNRS 7201, UPMC Univ Paris 06
4 Place Jussieu, Case courrier 42
75252 Paris Cedex 05 (France)
Fax: (+33) 144273841
E-mail: anna.proust@upmc.fr

[c] Dr. G. Bidan
INAC/DIR CEA-Grenoble, 17 rue des Martyrs
38054 Grenoble Cedex 9 (France)
Fax: (+33) 4 38785691
E-mail: gerard.bidan@cea.fr

[d] Prof. Dr. A. Proust
Institut Universitaire de France

Supporting information for this article is available on the WWW under http://dx.doi.org/10.1002/chem.200903336.

infra). Yet, covalent grafting offers advantages in terms of stability and structure control, and it is the approach we have chosen.

Choice of POM and that of grafting protocol are both central to the implementation of POM-based memories. The functionalization of Lindqvist-type POMs is still the most documented among the different families of POMs.[8] Thus bromo- and iodo-arylimido derivatives of $[Mo_6O_{19}]^{2-}$[36a] can be further derivatized by palladium-catalyzed Sonogashira[36b] or Heck[37] coupling reactions and a diazonium salt of a hybrid prepared in this way has been grafted onto silicon surfaces.[23,38] Another example is the covalent immobilization of a {TiW_5}-POM through alcoholysis of the Ti–OMe bond in $[MeOTiW_5O_{18}]^{3-}$ with alkanol-derivatized silicon surfaces.[39] Also surface micropatterning by a functionalized Anderson-type POM was very recently reported.[40]

Since redox properties of Keggin-type POMs are more tunable than those of Lindqvist-type species, we chose to functionalize Keggin-type POMs for covalent grafting on silicon surfaces. We thus report here the synthesis and characterization of $(NBu_4)_3[PW_9O_{34}(t\text{BuSiO})_3Ge(CH_2)_2CO_2H] \equiv (NBu_4)_3$**1a** (**1**), $(NBu_4)_3[PW_9O_{34}(t\text{BuSiO})_3Ge(CH_2)_2CONHCH_2C{\equiv}CH] \equiv (NBu_4)_3$**2a** (**2**), $(NBu_4)_4[PW_{11}O_{39}Ge(CH_2)_2CO_2H] \equiv (NBu_4)_4$**3a** (**3**), and $(NBu_4)_4[PW_{11}O_{39}Ge(CH_2)_2CONHCH_2C{\equiv}CH] \equiv (NBu_4)_4$**4a** (**4**), as well as preliminary results on their electrochemical behavior in solution and after grafting onto silicon surfaces. To our knowledge, no example of covalent grafting of Keggin-type POMs onto electrodes had been previously reported.

Results and Discussion

Synthesis: Direct functionalization of complete Keggin-type POMs is difficult, unlike their Lindqvist counterparts.[41] However lacunary species allow convenient synthesis of various functionalized Keggin-type POMs. In particular, lacunary Keggin-type polyoxotungstates react with organosilanes, -germanes, and -stannanes to afford a variety of hybrids containing one or several functional groups.[8] As we were primarily interested in compounds containing a single functional group, we chose to start from mono- and trivacant heteropolyoxotungstates. Whereas most trichlorosilanes react with $Na_8H[\beta\text{-A-}PW_9O_{34}]\cdot 24H_2O$ under phase-transfer conditions to give compounds of the type $(NBu_4)_3[\alpha\text{-A-}PW_9O_{34}(RSiO)_3(RSi)]$, the corresponding reaction with *t*BuSiCl$_3$ yields $(NBu_4)_3[\alpha\text{-A-}PW_9O_{34}(t\text{BuSiOH})_3]$, which then reacts cleanly with RECl$_3$ (E = Si, Ge) to give $(NBu_4)_3[\alpha\text{-A-}PW_9O_{34}(t\text{BuSiO})_3(RE)]$, in which R may be a reactive function.[42] Compound **1**, $(NBu_4)_3[PW_9O_{34}(t\text{BuSiO})_3Ge(CH_2)_2CO_2H]$, has been obtained by using this two-step procedure and subsequent coupling with propargylamine afforded $(NBu_4)_3[PW_9O_{34}(t\text{BuSiO})_3Ge(CH_2)_2CONHCH_2C{\equiv}CH]$ (**2**). Whereas trichlorosilanes react with monovacant POMs $[\alpha\text{-}XW_{11}O_{39}]^{n-}$ to yield disubstituted hybrid anions of the type $[\alpha\text{-}XW_{11}O_{39}\{O(SiR)_2\}]^{(n-4)-}$,[8] the corresponding reactions with trichloro-germanes/stannanes give monosubstituted derivatives of the type $[\alpha\text{-}XW_{11}O_{39}(ER)]^{(n-3)-}$ (E = Ge,[43,44] Sn[43]). We focused on organogermyl derivatives and prepared $(NBu_4)_4[PW_{11}O_{39}Ge(CH_2)_2CO_2H]$ (**3**) by reaction of $(NBu_4)_4[H_3PW_{11}O_{39}]$ with $Cl_3Ge(CH_2)_2CO_2H$ in homogeneous conditions, and then $(NBu_4)_4[PW_{11}O_{39}Ge(CH_2)_2CONHCH_2C{\equiv}CH]$ (**4**) by subsequent coupling with propargylamine. The tetramethylammonium salt of $[PW_{11}O_{39}Ge(CH_2)_2CO_2H]^{4-}$ has been recently reported; it was obtained from $K_7[PW_{11}O_{39}]\cdot 13H_2O$.[44]

Multinuclear (^{1}H, ^{13}C, ^{29}Si, ^{31}P, and ^{183}W) NMR spectroscopic characterization

*$(NBu_4)_3[PW_9O_{34}(t\text{BuSiO})_3Ge(CH_2)_2CO_2H]$ (**1**)*: The formation of $[PW_9O_{34}(t\text{BuSiO})_3Ge(CH_2)_2CO_2H]^{3-}$ (**1a**) by reaction of $[PW_9O_{34}(t\text{BuSiOH})_3]^{3-}$ with $Cl_3Ge(CH_2)_2CO_2H$ is conveniently monitored by ^{31}P NMR spectroscopy: the signal of **1a** ($\delta = -16.34$ ppm) is shifted to a lower frequency by approximately $\delta = 0.5$ ppm relative to that of the open-structure platform $[PW_9O_{34}(t\text{BuSiOH})_3]^{3-}$ ($\delta = -15.9$ ppm), which is consistent with a closed, that is, capped, structure.[42a] This conclusion is corroborated by {^{1}H}^{29}Si NMR spectroscopy which shows that the resonance of **1a** at $\delta = -58.34$ ppm (with tungsten satellites, ^2J(W-Si)≅8 Hz, see the Supporting Information, Figure S1) is shifted by more than $\delta = 10$ ppm relative to $[PW_9O_{34}(t\text{BuSiOH})_3]^{3-}$ ($\delta = -46.42$ ppm). Moreover, the observation of a single ^{29}Si NMR spectroscopic resonance points to equivalence of the three *t*BuSi groups.

The ^{1}H NMR spectrum of **1** (see the Supporting Information, Figure S2) exhibits the four multiplets from the tetrabutylammonium cations and three signals of the hybrid anion, that is, one singlet at $\delta = 0.99$ ppm (*t*Bu) and two AA′XX′ complex multiplets[45] centered at $\delta = 2.57$ and 1.55 ppm, which are assigned to the methylene groups adjacent to CO_2H and Ge, respectively. Note that because of overlapping with the strong NBu_4 multiplet centered at $\delta = 1.63$ ppm (24 H), observation and quantification of the last AA′XX′ system requires selective gated irradiation (homodecoupling experiment) at $\delta = 3.13$ ppm (see Figure S2c in the Supporting Information). Relative integration of the various multiplets agrees with the chemical formula, that is, three NBu_4^+ cations for one hybrid anion.

The {^{1}H}^{13}C NMR spectrum of **1a** displays five peaks at $\delta = 174.06$ (CO_2H), 27.07 (Me group of *t*Bu), 19.51 (C_Q of *t*Bu), 28.05, and 13.89 ppm (methylenic C). Consistently with the ^{1}H NMR spectra, the last signal, assigned to a CH_2 adjacent to Ge, is significantly shifted to a lower frequency with respect to $Cl_3Ge(CH_2)_2CO_2H$ ($\delta = 27.3$ ppm).

Finally, the ^{183}W NMR spectrum of **1a** displays two resonances in the intensity ratio 1:2 at $\delta = -79.4$ and -156.0 ppm, respectively (Figure 1). These chemical shift values and the homo- and heteronuclear coupling constants (^2J(W-W) = 22.4; ^2J(W-P) = ~0.8 and 1.4 Hz) do not differ markedly from the corresponding values for the open-structure platform $[PW_9O_{34}(t\text{BuSiO})_3]^{3-}$; this demonstrates again the relative rigidity of this platform. All together the NMR

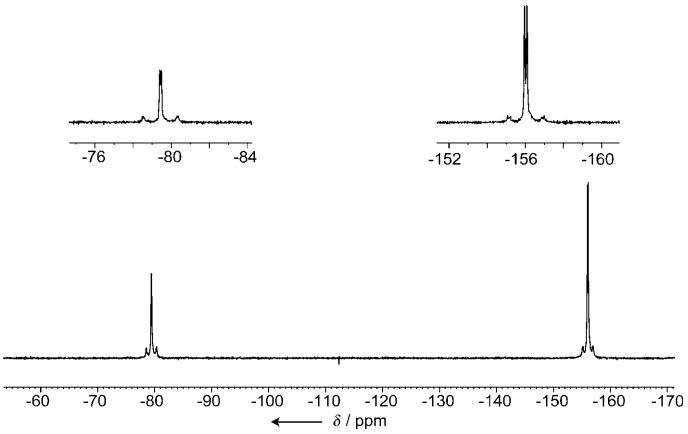

Figure 1. ^{183}W NMR spectrum of $[PW_9O_{34}(t\text{BuSiO})_3Ge(CH_2)_2CO_2H]^{3-}$ (**1a**) in DMF/CD_3COCD_3.

spectroscopic data show that in solution **1a** retains the ternary symmetry of the precursor (C_{3v}), which is consistent with the solid-state structure (vide infra).

*$(NBu_4)_3[PW_9O_{34}(t\text{BuSiO})_3Ge(CH_2)_2CONHCH_2C{\equiv}CH]$ (**2**)*: Whereas conversion of **1a** into **2a** does not shift the ^{31}P NMR spectroscopic signal ($\delta = -16.35$ ppm), the completion of the amide-coupling reaction can be demonstrated by ^{1}H NMR spectroscopy (Figure 2). Note that due to partial

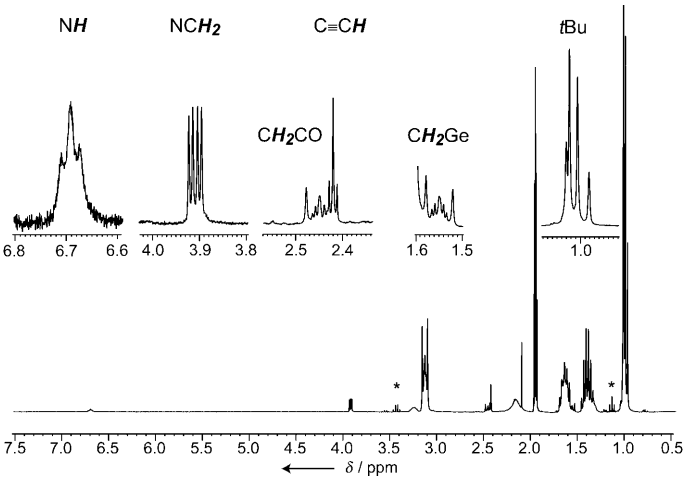

Figure 2. ^{1}H NMR spectrum of $(NBu_4)_3[PW_9O_{34}(t\text{BuSiO})_3Ge(CH_2)_2$-$CONHCH_2C{\equiv}CH]$ (**2**) in CD_3CN, with computer expansion of the hybrid anion resonances; expansion of the $\delta = 1.55$ ppm multiplet (CH_2 close to Ge) is part of a homodecoupled spectrum obtained with irradiation at $\delta = 3.13$ ppm, which reduces overlap with the strong NBu_4 signal at $\delta = 1.63$ ppm (* = diethyl ether).

overlapping with intense NBu_4 multiplets, some signals of the $Ge(CH_2)_2CONHCH_2C{\equiv}CH$ function could be detected and quantified only with the help of homodecoupling experiments. The amide and ethynyl protons give rise to triplets at $\delta = 6.69$ and 2.42 ppm, respectively, due to coupling with the propargylic protons (complex multiplet, $\delta = 3.91$ ppm). The signals from the *t*Bu groups (singlet, $\delta = 1.02$ ppm) and the methylene groups adjacent to CO and Ge (complex multiplets centered at $\delta = 2.45$ and 1.55 ppm, respectively) are nearly unaffected by the coupling. As for **1**, relative integration of the different multiplets is consistent with the chemical formula, that is, three NBu_4^+ cations for one hybrid anion. The IR spectra also consistently showed the disappearance of the $\nu(CO_2H)$ band at 1732 cm^{-1} and the appearance of the ν(C(O)NH) band at 1674 cm^{-1}.

*$(NBu_4)_4[PW_{11}O_{39}Ge(CH_2)_2CO_2H]$ (**3**)*: The ^{31}P NMR spectrum of $[PW_{11}O_{39}Ge(CH_2)_2CO_2H]^{4-}$ (**3a**) exhibits a signal at $\delta = -13.48$ ppm, shifted by $\delta = 1.1$ ppm to a lower frequency relative to that of the monovacant precursor $[H_2PW_{11}O_{39}]^{5-}$ ($\delta = -12.39$ ppm) This is consistent with our previous observations of the progressive increase of ^{31}P shielding on going from vacant to saturated P-centered POMs.[46,47]

Apart from the four multiplets from the tetrabutylammonium cations, the ^{1}H NMR spectrum of **3** exhibits one complex multiplet centered at $\delta = 2.62$ ppm that is assigned to the methylene group adjacent to CO_2H (see the Supporting Information, Figure S3). As the in case of **1**, this multiplet may arise from magnetic nonequivalence of the two protons (AA′XX′ system). According to integration, the signal from the methylene group adjacent to Ge is likely hidden under the strong NBu_4 signal at $\delta = 1.40$ ppm; this was indirectly demonstrated by a homodecoupling experiment with irradiation at $\delta = 1.40$ ppm, whereby the multiplet at $\delta = 2.62$ ppm reduced to a singlet.

The $\{^1H\}^{13}C$ spectrum of **3a** displays three low-intensity signals at $\delta = 176.77$ (COOH), 30.16, and 21.66 ppm (methylene groups). It should be noted that the signal assigned to the CH_2 attached to the germanium atom ($\delta = +21.66$ ppm) is shifted to a higher frequency by $\delta = 8$ ppm relative to that of **1a** ($\delta = 13.89$ ppm).

The ^{183}W NMR spectrum exhibits the expected six-line pattern of a monosubstituted Keggin derivative with overall C_s symmetry (see the Supporting Information, Figure S4). Whereas five lines are observed in a narrow δ range between $\delta = -90$ and -114 ppm, the sixth one is shifted to a low frequency at $\delta = -187.9$ ppm and should be assigned to one pair of W nuclei close to Ge. Full assignment of this spectrum will be discussed below, along with that of $[PW_{11}O_{39}Ge(CH_2)_2C(O)NHCH_2C{\equiv}CH]^{4-}$ (**4a**).

*$(NBu_4)_4[PW_{11}O_{39}Ge(CH_2)_2C(O)NHCH_2C{\equiv}CH]$ (**4**)*: The ^{31}P and ^{183}W NMR spectra of **4a** are very similar to those of **3a**. As in the case of the $[PW_9O_{34}(t\text{BuSiO})_3]^{3-}$ platform (vide supra) success of the amide-coupling reaction is demonstrated by ^{1}H NMR spectroscopy with the help of homodecoupling experiments (see the Supporting Information, Figure S5) Among the different signals from the anion, the amide and ethynyl protons give rise to triplets at $\delta = 6.84$ and 2.39 ppm, respectively, due to coupling with the propargyl protons (doublet of doublets, $\delta = 3.92$ ppm). The signals of the methylene groups adjacent to CO and Ge (AA′XX′ multiplets centered at $\delta = 2.48$ and $\delta = 1.35$ ppm,

respectively) are slightly shifted to a lower frequency relative to that of **3a**.

The $\{^1H\}^{13}C$ NMR spectrum of **4a** is characterized by six peaks at 174.39 (***C***O), 81.85 (***C***≡CH), 71.50 (C≡***C***H), 31.60 (***C***H_2CO), 29.29 (N***C***H_2), and 21.74 (Ge***C***H_2).

As already noted, the ^{183}W NMR spectrum of **4a** is quite similar to that of **3a**. It displays six doublets with relative integrated intensity ratio 2:2:2:1:2 in agreement with an overall C_s symmetry of the POM framework. Under ^{31}P decoupling all doublets become narrow singlets (Figure 3). Ob-

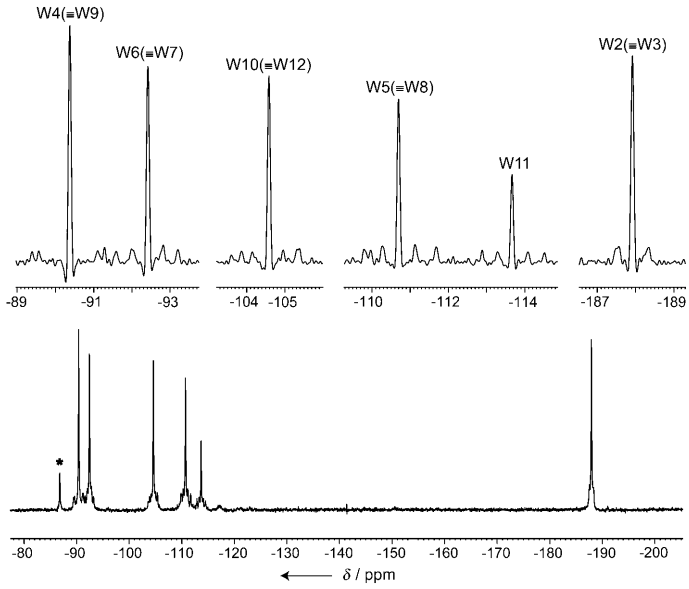

Figure 3. $\{^{31}P\}^{183}W$ NMR spectrum of $[PW_{11}O_{39}Ge(CH_2)_2C(O)NHCH_2C{\equiv}CH]^{4-}$ (**4a**) in DMF/CD_3CN. Bottom: full spectrum after apodization of the FID by exponential function before Fourier transform (the small peak marked by an asterisk at $\delta = -86.8$ ppm corresponds to less than 3% of $PW_{12}O_{40}^{3-}$ impurity). Top: abscissa expansion of the six resonances after resolution enhancement through the Gaussian function to show the tungsten satellites.

servation of well-defined tungsten satellites allows accurate measurement of the homonuclear $^2J_{W-W}$ coupling constants and determination of tungsten–tungsten connectivity. The results of the assignments are given in Table 1 (see the Supporting Information for an explanation of the strategy). The atom numbering is given according to IUPAC convention[48] with Ge at position 1 (Figure 4).

As the linker could influence the electronic interaction between the surface and the POM subunit in surface-grafted POMs, it is worth comparing the ^{183}W NMR spectroscopic

Table 1. Comparison of the ^{183}W chemical shifts [ppm] for $[PW_{11}O_{39}\{O(SiEt)_2\}]^{3-}$, $[PW_{11}O_{39}Ge(CH_2)_2C(O)NHCH_2C{\equiv}CH]^{4-}$ (**4a**), and $[PW_{11}O_{39}\{Sn(CH_2)_2CO_2H\}]^{4-}$.

	$[PW_{11}O_{39}\{O(SiEt)_2\}]^{3-}$[49]	**4a**	$[PW_{11}O_{39}\{Sn(CH_2)_2CO_2H\}]^{4-}$[50]
W2(≡W3)	−251.5	−187.9	−165.1
W4(≡W9)	−198.7	−90.3	−71.4
W5(≡W8)	−121.8	−110.7	−115.5
W6(≡W7)	−99.0	−92.4	−93.0
W10(≡W12)	−104.0	−104.6	−113.2
W11	−108.0	−113.7	−127.6

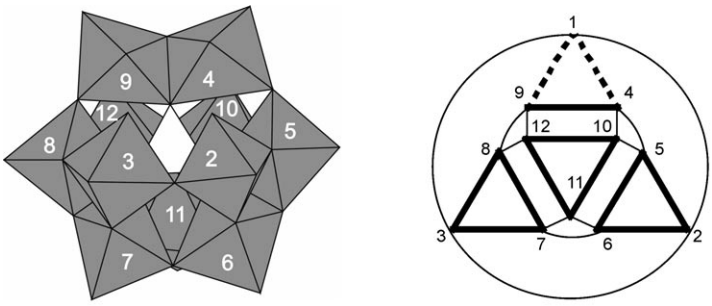

Figure 4. Representation of the POM framework of **3** and **4** with atom numbering according to IUPAC convention.[48] Left: polyhedral representation with Ge omitted for clarity. Right: schematic plane representation, —— and —— hold for intra- and intertrimetallic group W-O-W junctions, respectively (----- represent Ge-O-W junctions).

data for structurally related POMs with different linkers, namely organosilyl, -germyl and -stannyl groups. Derivatives of the monovacant tungstophosphate allow such a comparison (Table 1), even if the structure of the Si species $[PW_{11}O_{39}\{O(SiR)_2\}]^{3-}$ differ from those of Ge and Sn species $[PW_{11}O_{39}(ER)]^{4-}$ (E = Ge, Sn) by the nature of the grafted fragment, that is, a dimeric RSi–O–SiR or a monomeric ER group, respectively.

For the three derivatives, the resonances of the tungsten nuclei remote from the substituent are observed in a very narrow δ range spanning less than $\delta = 30$ ppm. For the remaining nuclei, that is, W2(≡W3) and W4(≡W9), there are large differences between the three species. The most shielded nuclei are always W2(≡W3), which are connected via corners to the substituting element. This agrees with previous observations made by Domaille on various monosubstituted Keggin-type polyoxotungstates.[51] Shielding of the W2(≡W3) nuclei decreases along the series Si ≫ Ge > Sn. A similar sequence is observed for W4(≡W9), which are connected via edges to the substituting element. In the case of the tin and germanium compounds, the W4(≡W9) pair is the least shielded of all the tungsten nuclei. A more detailed comparison of the ^{183}W NMR spectroscopic data of the three derivatives including homonuclear coupling constants is presented in the Supporting Information.

Crystal structure of $(NBu_4)_3[PW_9O_{34}(t\text{BuSiO})_3Ge(CH_2)_2CO_2H]\cdot H_2O$: Colorless crystals of **1**·H_2O were obtained upon slow evaporation of a solution of **1** in DMF in air at room temperature. They belong to the trigonal *R*3c space group. The asymmetric unit contains one tetrabutylammonium cation, one third of the anion, located at a C_3 axis, going through O(11), P(1), Ge(1), and C(5), and a water molecule H-bonded to the carboxylic acid function. A disorder model has been introduced for the $CH_2CH_2CO_2H$ and the *tert*-butyl groups (see the Experimental Section). The overall molecular structure of the anion (Figure 5) is similar to that of other derivatives of the type $[\alpha\text{-A-}PW_9O_{34}(RSiO)_3(RSi)]^{3-}$.[42b,52] The W–O bond lengths fall in the range expected for terminal- (1.711(11) to 1.744(11) Å), doubly- (1.871(11) to 1.965(12) Å), and triply-bridging oxo ligands

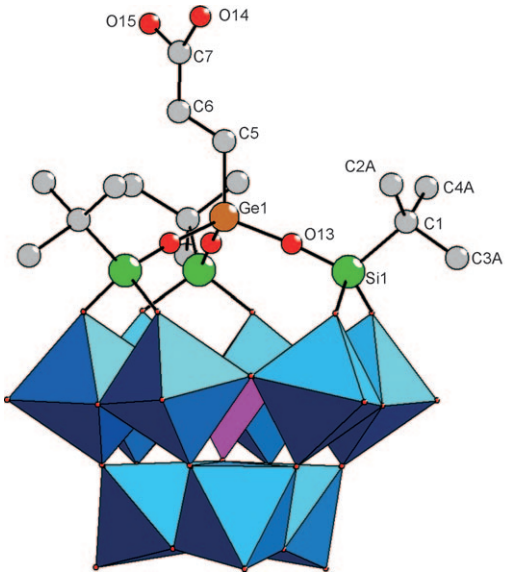

Figure 5. Mixed polyhedral and ball-and-stick representation of $[PW_9O_{34}(t\text{BuSiO})_3Ge(CH_2)_2CO_2H]^{3-}$ (**1a**).

(2.358(10) to 2.402(10) Å). The Ge(1)–O(13) distance of 1.822(14) Å is consistently longer than the Si(1)–O(13) distance of 1.558(15) Å.

Electrochemical studies:

*Electrochemical characterization of $(NBu_4)_3[PW_9O_{34}(tBuSiO)_3Ge(CH_2)_2CO_2H]$ (**1**) and $(NBu_4)_3[PW_9O_{34}(tBuSiO)_3Ge(CH_2)_2CONHCH_2C{\equiv}CH]$ (**2**) in solution*: We have investigated the electrochemical behavior of the organogermyl species **1a** and **2a** by cyclic voltammetry in acetonitrile at a glassy carbon electrode, by using NBu_4BF_4 as the supporting electrolyte. Representative cyclic voltammograms for $(NBu_4)_3$**1a** and $(NBu_4)_3$**2a** are shown in Figure 6 together with that of $(NBu_4)_3[PW_9O_{34}(t\text{BuSiOH})_3]$ for comparison. It must be pointed out that the voltammograms of **1a** and **2a** were obtained after repeated cycles between 0 and −2.5 V, whereas the initial voltammograms displayed an additional feature that progressively disappeared under cycling (see the Supporting Information, Figure S6 and S7; electrochemical data are gathered in Table 2). Each of the three polyoxotungstate hybrids $[PW_9O_{34}(t\text{BuSiOH})_3]^{3-}$, **1a** and **2a**, displays three reversible waves. They correspond to one-electron redox processes as it is known to be the case for Keggin-type POMs in nonaqueous solvents when no protonation accompanies reduction.[53,54] The reduction waves of **1a** and **2a** are only slightly shifted to more negative potentials with respect to $[PW_9O_{34}(t\text{BuSiOH})_3]^{3-}$.

Table 2. Electrochemical data.[a]

Compound	Process	E_{pa}[b]	E_{pc}[b]	$^1/_2(E_{pa}+E_{pc})$[b]	$E_{pa}-E_{pc}$[c]
$[PW_9O_{34}(t\text{BuSiOH})_3]^{3-}$	I	−0.619	−0.671	−0.645	52
	II	−1.103	−1.155	−1.129	52
	III	−1.793	−1.845	−1.819	52
1a	I	−0.756	−0.798	−0.777	42
	II	−1.220	−1.284	−1.252	64
	III	−1.891	−1.976	−1.933	85
2a	I	−0.692	−0.745	−0.718	53
	II	−1.173	−1.237	−1.205	64
	III	−1.841	−1.918	−1.879	77

[a] $c=1\times10^{-3}$ mol L^{-1} in acetonitrile, 0.1 mol L^{-1} NBu_4BF_4, 20 mV s^{-1}. [b] V vs. SCE. [c] mV.

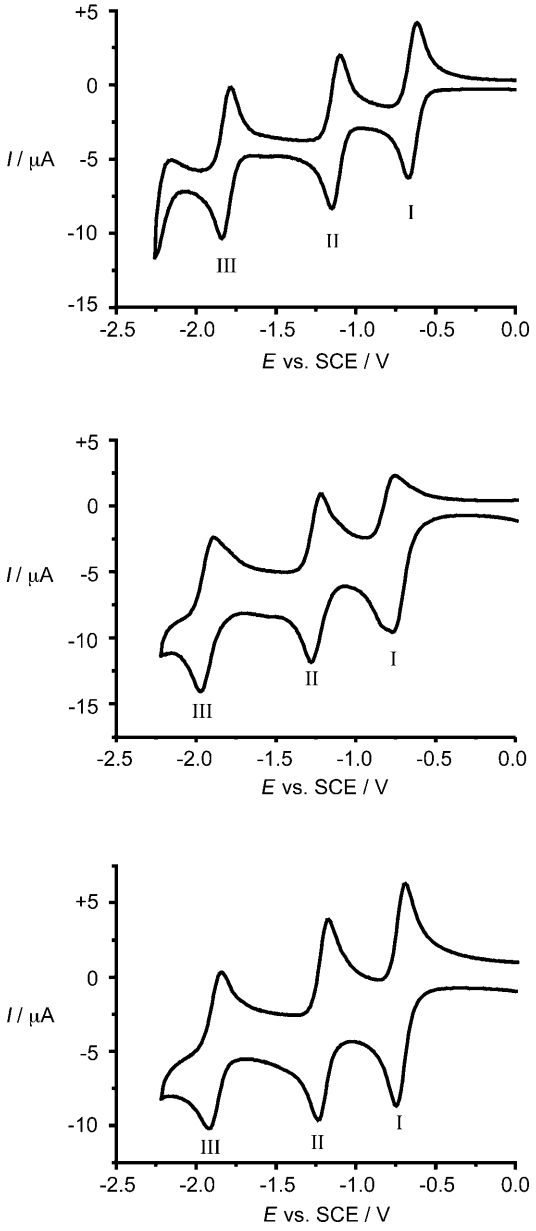

Figure 6. Cyclic voltammograms of $(NBu_4)_3[PW_9O_{34}(t\text{BuSiOH})_3]$ (top), $(NBu_4)_3[PW_9O_{34}(t\text{BuSiO})_3Ge(CH_2)_2CO_2H]$ (**1**) (middle), and $(NBu_4)_3[PW_9O_{34}(t\text{BuSiO})_3Ge(CH_2)_2CONHCH_2{-}C{\equiv}CH]$ (**2**) (bottom) at a glassy carbon electrode. ([POM] $=1\times10^{-3}$ mol L^{-1} in acetonitrile, 0.1 mol L^{-1} NBu_4BF_4, 20 mV s^{-1}).

Electrochemical grafting onto silicon substrates: Electrografting of **2a** onto an n-type highly doped Si surface was achieved by passing an anodic current through a solution of

$(NBu_4)_3$**2a** (1 mmol L^{-1}) and NBu_4BF_4 (0.1 mol L^{-1}) in CH_3CN, by using a protocol adapted from the literature[55] and schematically represented in Scheme 1. The cyclic voltammograms obtained in a three-electrode cell made up of the POM-modified Si electrode as the working electrode

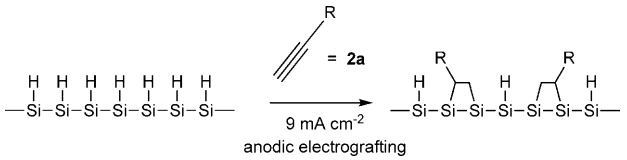

Scheme 1. Schematic representation of the electrografting procedure utilized in this paper.[55a]

and platinum reference and counter electrodes are shown in Figure 7. Three quasi-reversible redox processes are observed with formal potentials of −0.51, −0.93, and −1.38 V versus Pt wire. They are reminiscent of those observed for **2a** in solution, although they are less well-resolved, and thus are assigned to successive reductions of W centers. The working electrode potential was scanned from the lower to higher limit and back at scan rates varying from 20 to 500 mV s^{-1}. The second cathodic peak current (II) shows a linear dependence on the scan rate (see Figure 7 inset), which indicates that the electroactive species are indeed surface-confined. For immobilized species, the theoretical potential difference value between the anodic and cathodic peaks should be zero. The observed value of 80 mV at the scan rate of 500 mV s^{-1} could be interpreted as a slower charge transfer at the Si surface due to the organic spacer. An increase of the potential difference between peaks with the spacing arm length is classically observed in SAMs made of redox species attached at the end of an alkyl chain.[56] These electrochemical results indicate that the POM-modified Si is electrochemically active. There is no evidence for a limited electron transfer between the clusters

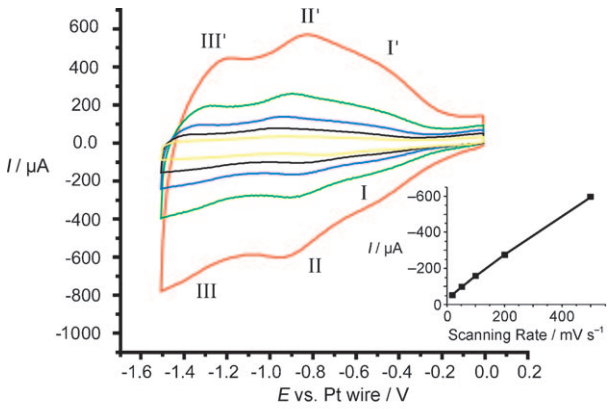

Figure 7. Cyclic voltammograms at the POM-Si modified electrode at different scan rates: 20, 50, 100, 200, 500 mV s^{-1} (acetonitrile, 0.1 mol L^{-1} Bu_4NBF_4). Inset) Linear dependency of peak II current on scan rate.

and the Si substrate contrary to covalently grafted organoimido hexamolybdates on p-type Si wafers.[38]

Conclusion

New organosilyl/-germyl Keggin-type polyoxotungstates have been synthesized for covalent grafting onto Si surfaces. They were characterized by multinuclear NMR spectroscopy and cyclic voltammetry, and, for one of them, by single-crystal X-ray diffraction. Electrografting of $[PW_9O_{34}(t\text{BuSiO})_3Ge(CH_2)_2CONHCH_2{-}C{\equiv}CH]^{3-}$ has been achieved on n-type Si(100) wafers and the resulting films proved to be electrochemically active. Such materials are promising components for the design of multilevel molecular memories.

Experimental Section

General: $(NBu_4)_3[PW_9O_{34}(t\text{BuSiOH})_3]$,[42a] $(NBu_4)_4[H_3PW_{11}O_{39}]$,[57] and $Cl_3Ge(CH_2)_2CO_2H$[43] were prepared as described in the literature and their purity was checked by ^{31}P and ^1H NMR spectroscopy. Unless otherwise noted, all the chemical compounds were purchased from Aldrich. Sulfuric acid (H_2SO_4, 96%), hydrogen peroxide (30%), hydrofluoric acid (1%), acetone, ethanol, and dichloromethane were used as received. Acetonitrile was dried and freshly distilled over CaH_2 before use. NBu_4BF_4 was dried overnight under vacuum at 110 °C. Elemental analyses were performed by the Service de Microanalyses (Université Pierre et Marie Curie) and the Laboratoire Central d'Analyse of the CNRS (Vernaison, France).

Methods

IR spectroscopy: IR spectra were obtained as KBr pellets on a Bio-Rad Win-IR FTS 165 FTIR spectrophotometer.

NMR spectroscopy: The ^1H (300.13 MHz), $\{^1H\}^{13}C$ (75.5 MHz), and $\{^1H\}^{31}P$ (121.5 MHz) NMR spectra were obtained at room temperature in 5 mm o.d. tubes on a Bruker AvanceII 300 spectrometer equipped with a QNP probehead. The $\{^1H\}^{29}Si$ (59.6 MHz) and ^{183}W (12.5 MHz) NMR spectra were recorded in 10 mm o.d. tubes on the Bruker AvanceII 300 spectrometer equipped with a tunable BBO probehead and a special low-frequency VSP probehead, respectively. For ^1H and ^{13}C NMR spectra, chemical shifts are referenced with respect to TMS ($SiMe_4$) by using the solvent signals as secondary standard (CHD_2CN: $\delta(^1H)=1.94$, $\boldsymbol{C}D_3CN$: $\delta(^{13}C)=1.32$, $\boldsymbol{C}D_3CO\boldsymbol{C}D_3$: $\delta(^{13}C)=29.84$ ppm).[58] For other nuclei, chemical shifts were measured by the substitution method and they are given with respect to TMS (^{29}Si), 85% H_3PO_4 (^{31}P), and to external alkaline 2 M Na_2WO_4 aqueous solution (^{183}W), respectively. For ^{183}W, a saturated aqueous solution of $H_4SiW_{12}O_{40}$ was used as secondary standard ($\delta=-103.8$ ppm).[59]

Electrochemistry: All electrochemical measurements were performed at room temperature under argon in a standard three-electrode cell connected to an Autolab PGSTAT100 potentiostat (Eco Chemie BV) equipped with general-purpose electrochemical system software. Freshly cleaned glassy carbon and Pt electrodes (3 mm diameter) were used as the working and auxiliary electrode, respectively. A Pt wire served as the pseudo-reference electrode. Ferrocene (Fc) was added to the solutions as an internal standard. Potentials are given with respect to aqueous SCE ($E_{Fc^+/Fc}=+0.415$ V vs. SCE).

Si surface preparation: The single-crystal phosphorous-doped Si(100) wafers were polished and sliced into rectangular strips of about 0.5 × 1.5 cm^2 in size. A 0.4 × 0.5 cm^2 Cr/Au top contact layer (thickness: 25 nm/500 nm) was deposited on the silicon substrate electrode for cyclic voltammetry measurements. n-Si (phosphorus-doped, two-sides polished, 8×10^{-3}–2.2×10^{-2} Ω cm resistivity) electrodes were used for the experiments.

To remove the organic residues on the surface, the Si(100) wafers were immersed in a 96 wt.% mixture of concentrated 70% H_2SO_4 and 30% H_2O_2 (piranha solution) for about 30 s. After rinsing with copious amounts of water, the Si(100) wafers were blow-dried with purified argon and then immersed in 1% HF for 1 min to remove the oxide film and to leave behind a hydrogen-ended wafer.

Electrografting: Electrografting was performed in a three-electrode cell placed inside a N_2-purged dry-box (Plas Labs). The working electrode was a hydrogenated n-Si wafer with an area of 0.75 cm^2, exposing a 0.45 cm^2 area (for both sides a total area of 0.9 cm^2), in a solution of the reactant ($(NBu_4)_3$**2a**, 0.1 mmol L^{-1}) and the supporting electrolyte (NBu_4BF_4, 0.1 mol L^{-1}) in CH_3CN. Platinum reference and counter electrodes were used. Electrografting was carried out at a constant anodic-current density of 9 mA cm^{-2} for 10^3 s. Following completion of the reaction, the sample was rinsed with CH_3CN, ultrasonicated in CH_3CN for 3 min (×3), to remove any adsorbed species, and dried under a flow of argon. The POM-modified Si surface was characterized by cyclic voltammetry, by using a solution of NBu_4BF_4 in CH_3CN (0.1 mol L^{-1}) and platinum reference and counter electrodes.

Syntheses

*$(NBu_4)_3[PW_9O_{34}(tBuSiO)_3Ge(CH_2)_2CO_2H]$ (**1**)*: An excess of $Cl_3Ge(CH_2)_2CO_2H$ (0.801 g, 3.170 mmol) was added to a solution of $(NBu_4)_3[PW_9O_{34}(tBuSiOH)_3]$ (2.016 g, 0.633 mmol) in dry acetonitrile (80 mL). The reaction mixture was kept overnight at room temperature, then the solvent was removed in vacuo after checking for completion of the reaction by ^{31}P NMR spectroscopy. The residue was dissolved in acetone (10 mL) and compound **1** was precipitated by the addition of a mixture of diethyl ether and ethanol (10:1), filtered off, and dried in air (1.8 g, 83%). Colorless crystals of **1**·H_2O, suitable for single-crystal X-ray crystallography, were grown from a DMF solution by slow evaporation in air at room temperature. IR (KBr): $\tilde{\nu}$ = 2963 (m), 2935 (m), 2876 (w), 2860 (w), 1732 (w), 1677 (w), 1487 (m), 1475 (s), 1384 (w), 1107 (s), 1036 (m), 974 (s), 951 (s), 866 (s), 806 (s), 726 (m), 603 (w), 580 (w), 530 (w), 505 (w), 482 (w), 425 (w), 391 (m), 363 cm^{-1} (m); ^{31}P NMR (CD_3CN): δ = −16.34 ppm; ^1H NMR (CD_3CN): δ = 0.98 (t, 36H; $NCH_2CH_2CH_2C\mathbf{H_3}$), 0.99 (s, 27H; *t*Bu), 1.40 (sextet, 24H; $NCH_2CH_2C\mathbf{H_2}CH_3$), 1.55 (m, 2H; $GeC\mathbf{H_2}CH_2COOH$), 1.63 (m, 24H; $NCH_2C\mathbf{H_2}CH_2CH_3$), 2.57 (m, 2H; $GeCH_2C\mathbf{H_2}COOH$), 3.13 ppm (m, 24H; $NC\mathbf{H_2}CH_2CH_2CH_3$); ^{13}C NMR (DMF, CD_3COCD_3): δ = 13.78 ($NCH_2CH_2CH_2\mathbf{C}H_3$), 13.89 ($GeCH_2CH_2CO_2H$), 19.51 ($\mathbf{C}(CH)_3$), 20.03 ($(NCH_2CH_2\mathbf{C}H_2CH_3$), 24.11 ($NCH_2\mathbf{C}H_2CH_2CH_3$), 27.07 ($C(\mathbf{C}H_3)_3$), 28.05 ($GeCH_2\mathbf{C}H_2COOH$), 58.78 ($N\mathbf{C}H_2CH_2CH_2CH_3$), 174.06 ppm ($GeCH_2CH_2\mathbf{C}OOH$); ^{29}Si NMR (DMF, CD_3COCD_3): δ = −58.34 ppm ($^2J_{W-Si}$ = 8 Hz); ^{183}W NMR (DMF, CD_3COCD_3): δ = −156.0 (d, 6W, $^2J_{W-P}$ = 1.4, $^2J_{W-W}$ = 22.4 Hz), −79.4 ppm (d, 3W, $^2J_{W-P}$ = 0.8, $^2J_{W-W}$ = 22.4 Hz); elemental analysis calcd (%) for $C_{63}H_{140}GeN_3PO_{39}Si_3W_9$ (3406.28): C 22.21, H 4.14, Ge 2.13, N 1.23, P 0.91, Si 2.47, W 48.58; found: C 22.37, H 3.96, Ge 1.66, N 1.30, P 0.95, Si 2.44, W 46.77.

$(NBu_4)_3[PW_9O_{34}(tBuSiO)_3Ge(CH_2)_2C(O)NHCH_2C{\equiv}CH]$ (**2**): Triethylamine (43 μL, 0.307 mmol), isobutylchloroformiate (40 μL, 0.307 mmol), and, after 25 min, propargylamine (36 μL, 0.521 mmol) were added successively to a solution of $(NBu_4)_3[PW_9O_{34}(tBuSiO)_3Ge(CH_2)_2CO_2H]$ (**1**) (0.888 g, 0.261 mmol) in dry acetonitrile (10 mL). The solution was stirred overnight and then evaporated to dryness. The residue was dissolved in acetone (10 mL) and compound **2** was precipitated by the addition of a mixture of diethyl ether and ethanol (10:1), filtered off, and dried in air (0.67 g, 74%). IR (KBr): $\tilde{\nu}$ = 2963 (m), 2935 (m), 2877 (w), 2860 (w), 1674 (w), 1485 (m), 1474 (s), 1384 (w), 1107 (s), 1037 (m), 973 (s), 951 (s), 865 (s), 807 (s), 726 (m), 603 (w), 580 (w), 530 (w), 506 (w), 482 (w), 452 (w), 392 (m), 364 cm^{-1} (m); ^{31}P NMR (CD_3CN): δ = −16.35 ppm; ^1H NMR (CD_3CN): δ = 0.98 (t, 36H; $NCH_2CH_2CH_2C\mathbf{H_3}$), 1.02 (s, 27H; *t*Bu), 1.39 (sextet, 24H; $NCH_2CH_2C\mathbf{H_2}CH_3$), 1.55 (m, 2H; $GeC\mathbf{H_2}CH_2C(O)NHCH_2C{\equiv}CH$), 1.63 (m, 24H; $NCH_2C\mathbf{H_2}CH_2CH_3$), 2.42 (t, 1H, $^4J_{H-H}$ = 2.54 Hz; $GeCH_2CH_2C(O)NHCH_2C{\equiv}C\mathbf{H}$,), 2.45 (m, 2H; $GeCH_2C\mathbf{H_2}C(O)NHCH_2C{\equiv}CH$), 3.13 (m, 24H; $NC\mathbf{H_2}CH_2CH_2CH_3$), 3.91 (dd, 2H, $^3J_{H-H}$ = 5.56, $^4J_{H-H}$ = 2.53 Hz; $GeCH_2CH_2C(O)NHC\mathbf{H_2}C{\equiv}CH$), 6.69 ppm (brt, 1H, $^3J_{H-H}$ ≈ 5.6 Hz); elemental analysis calcd (%) for $C_{66}H_{143}GeN_4PO_{38}Si_3W_9$ (3443.35): C 23.02, H 4.19, Ge 2.11, N 1.63, Si 2.45, W 48.05; found: C 22.60, H 4.27, Ge 1.94, N 1.65, Si 2.93, W 48.25.

*$(NBu_4)_4[PW_{11}O_{39}Ge(CH_2)_2CO_2H]$ (**3**)*: $Cl_3Ge(CH_2)_2COOH$ (0.250 g, 0.992 mmol) and triethylamine (210 μL, 1.505 mmol) were added successively to a solution of $(NBu_4)_4[H_3PW_{11}O_{39}]$ (4 g, 1.096 mmol) in dry acetonitrile (160 mL). The solution was stirred for 5 h and then evaporated to dryness. The residue was dissolved in acetone (10 mL). The white product that precipitated by addition of a mixture of diethyl ether and ethanol (10:1) was filtered off and dried in air (3.9 g). It proved to be a mixed NEt_3H^+/NBu_4^+ salt on the basis of ^1H and ^{13}C NMR spectroscopic analyses. Analytically pure NBu_4^+ salt (**3**) was obtained by recrystallization in DMF. IR (KBr): $\tilde{\nu}$ = 2963 (m), 2935 (m), 2875 (w), 1654 (w), 1485 (m), 1382 (w), 1099 (m), 1072 (s), 963 (s), 886 (s), 808 (s), 738 (sh), 519 (w), 389 cm^{-1} (s); ^{31}P NMR (CD_3CN): δ = −13.48 ppm; ^1H NMR (CD_3CN): δ = 0.99 (t, 48H; $NCH_2CH_2CH_2C\mathbf{H_3}$), 1.40 (m, 34H; $NCH_2CH_2C\mathbf{H_2}CH_3 + GeC\mathbf{H_2}CH_2COOH$), 1.65 (m, 32H; $NCH_2C\mathbf{H_2}CH_2CH_3$), 2.62 (m, 2H; $GeCH_2C\mathbf{H_2}COOH$), 3.15 ppm (m, 32H; $NC\mathbf{H_2}CH_2CH_2CH_3$); ^{13}C NMR (DMF, CD_3CN): δ = 9.66 ($NCH_2\mathbf{C}H_3$), 14.42 ($NCH_2CH_2CH_2\mathbf{C}H_3$), 20.64 ($(NCH_2CH_2\mathbf{C}H_2CH_3$), 21.66 ($GeCH_2CH_2COOH$), 24.72 ($NCH_2\mathbf{C}H_2CH_2CH_3$), 30.16 ($GeCH_2\mathbf{C}H_2COOH$), 47.40 ($N\mathbf{C}H_2CH_3$), 59.26 ($N\mathbf{C}H_2CH_2CH_2CH_3$), 176.77 ppm ($GeCH_2CH_2\mathbf{C}OOH$); ^{183}W NMR (DMF, CD_3CN): δ = −187.9 (2W, $^2J_{W-P}$ ≈ 1.2 Hz), −113.8 (1W, $^2J_{W-P}$ ≈ 1.3 Hz), −110.5 (2W, $^2J_{W-P}$ ≈ 0.9 Hz), −104.5 (2W, $^2J_{W-P}$ ≈ 1.1 Hz), −92.4 (2W, $^2J_{W-P}$ ≈ 1.2 Hz), −90.4 ppm (2W, $^2J_{W-P}$ ≈ 1.5 Hz); elemental analysis calcd (%) for $C_{67}H_{149}GeN_4PO_{41}W_{11}$ (3792.85): C 21.22, H 3.96, Ge 1.91, N 1.48, P 0.82, W 53.32; found: C 21.14, H 3.67, Ge 1.46, N 1.67, P 0.96, W 52.45.

*Synthesis of $(NBu_4)_4[PW_{11}O_{39}Ge(CH_2)_2C(O)NHCH_2C{\equiv}CH]$ (**4**)*: Triethylamine (81 μL, 0.630 mmol), isobutylchloroformiate (87 μL, 0.630 mmol), and, after 25 min, propargylamine (72 μL, 1.050 mmol) were added successively to a solution of $(NBu_4)_4[PW_{11}O_{39}Ge(CH_2)_2COOH]$ (**3**) (2 g, 0.53 mmol) in dry acetonitrile (20 mL). The solution was stirred overnight, filtered, and then evaporated to dryness. The residue was redissolved in acetone (10 mL) and compound **4** was precipitated by the addition of a mixture of diethyl ether and ethanol (10:1), filtered off, and dried in air (1.8 g, 89%). IR (KBr): $\tilde{\nu}$ = 2963 (m), 2937 (m), 2875 (w), 1668 (w), 1485 (m), 1382 (w), 1100 (m), 1072 (s), 963 (s), 886 (s), 807 (s), 518 (w), 506 (sh), 388 cm^{-1} (s); ^{31}P NMR (CD_3CN): δ = −13.50 ppm (−12.81 impurity 15%); ^1H NMR (CD_3CN): δ = 0.99 (t, 48H; $NCH_2CH_2CH_2C\mathbf{H_3}$), 1.41 (sextet, 32H; $NCH_2CH_2C\mathbf{H_2}CH_3$), 1.35 (m, 2H; $GeC\mathbf{H_2}CH_2C(O)NHCH_2C{\equiv}CH$), 1.65 (m, 32H; $NCH_2C\mathbf{H_2}CH_2CH_3$), 2.39 (t, 1H, $^4J_{H-H}$ = 2.55 Hz; $GeCH_2CH_2C(O)NHCH_2C{\equiv}C\mathbf{H}$), 2.48 (m, 2H; $GeCH_2C\mathbf{H_2}C(O)NHCH_2C{\equiv}CH$), 3.17 (m, 32H; $NC\mathbf{H_2}CH_2CH_2CH_3$), 3.92 (dd, 2H, $^3J_{H-H}$ = 5.59, $^4J_{H-H}$ = 2.47 Hz; $GeCH_2CH_2C(O)NHC\mathbf{H_2}C{\equiv}CH$), 6.84 ppm (brt, 1H, $^3J_{H-H}$ ≈ 5.4 Hz); ^{13}C NMR (CD_3CN): δ = 13.98 ($NCH_2CH_2CH_2\mathbf{C}H_3$), 21.74 ($GeC\mathbf{H_2}CH_2C(O)NHCH_2C{\equiv}CH$), 20.49 ($(NCH_2CH_2\mathbf{C}H_2CH_3$), 24.49 ($NCH_2\mathbf{C}H_2CH_2CH_3$), 29.29 ($GeCH_2CH_2C(O)NH\mathbf{C}H_2C{\equiv}CH$), 31.60 ($GeCH_2\mathbf{C}H_2C(O)NHCH_2C{\equiv}CH$), 59.37 ($N\mathbf{C}H_2CH_2CH_2CH_3$), 71.50 ($GeCH_2CH_2C(O)NHCH_2C{\equiv}\mathbf{C}H$), 81.85 ($GeCH_2CH_2C(O)NHCH_2\mathbf{C}{\equiv}CH$), 174.39 ppm ($GeCH_2CH_2\mathbf{C}(O)NHCH_2C{\equiv}CH$); ^{183}W NMR (DMF, CD_3CN): δ = −187.9 (d, 2W, $^2J_{W-P}$ = 1.5, $^2J_{W-W}$ = 10.7, 8.8 Hz), −113.7 (d, 1W, $^2J_{W-P}$ = 1.4, $^2J_{W-W}$ = 20.4, 9.9 Hz), −110.7 (d, 2W, $^2J_{W-P}$ = 1.2, $^2J_{W-W}$ = 23.6, 21.4, 10.6 Hz (2W)), −104.6 (d, 2W, $^2J_{W-P}$ = 1.1, $^2J_{W-W}$ = 21.4, 19.1, ca. 10 Hz), −92.4 (d, 2W, $^2J_{W-P}$ = 1.3, $^2J_{W-W}$ = 20.2, ca. 10 Hz (2W)), −90.3 ppm (d, 2W, $^2J_{W-P}$ = 1.6, $^2J_{W-W}$ = 23.5, 19.2 Hz); elemental analysis calcd (%) for $C_{70}H_{152}GeN_5PO_{40}W_{11}$ (3829.91): C 21.95, H 4.00, Ge 1.90, N 1.83, P 0.81, W 52.80; found: C 21.18, H 3.56, Ge 1.66, N 1.87, P 0.91, W 52.35.

X-ray diffraction study: Crystal data for $(NBu_4)_3[PW_9O_{34}(tBuSiO)_3Ge(CH_2)_2CO_2H]\cdot H_2O$ (**1**·H_2O): $C_{63}H_{140}GeN_3PO_{39}Si_3W_9$; M = 3424.28; colorless crystals; trigonal; space group = $R\bar{3}c$; a = b = 22.284(4), c = 36.880(6) Å; $\alpha = \beta = 90$, $\gamma = 120°$; U = 15860(5) $Å^3$; Z = 6; T = 200(2) K; μ = 10.15 mm^{-1}; 23428 reflections measured, 7333 independent (R_{int} = 0.046), 5525 observed with $I > 2\sigma(I)$, 375 variables refined, final R indices R_1 [$I > 2\sigma(I)$] = 0.0386 and wR_2 (all data) = 0.1161; GOF on F^2 = 1.21; max/min residual electron density = 2.819/−3.025 e $Å^{-3}$. Measurements were performed with a Bruker-Nonius Kappa-CCD diffractometer by using graphite-monochromated $Mo_{K\alpha}$ radiation. Unit-cell parameter de-

termination, data collection strategy, and integration were carried out with the Nonius EVAL-14 suite of programs.[60] The data were corrected from absorption by a multiscan method.[61] The structure was solved by direct methods by using the SHELXS-97 program and refined anisotropically by full-matrix least-squares on F^2 by using the SHELXL-97 software package.[62] Graphics were carried out by using DIAMOND.[63] All non-H atoms, except those of the pending $CH_2CH_2CO_2H$ on the anion, were refined anisotropically. Hydrogen atoms of the cation were introduced at calculated positions and refined isotropically. $CH_2CH_2CO_2H$ is disordered due to the three-fold axis: its geometry was restrained and isotropic displacement parameters of the oxygen atoms were fixed at 0.18, slightly above that of the carbon atom to which they are attached (0.17). The three terminal methyl groups of the *t*Bu group are also disordered over two equally occupied positions. The displacement parameters of related carbon atoms have consequently been fixed to be equal. CCDC-705019 contains the supplementary crystallographic data for this paper. These data can be obtained free of charge from The Cambridge Crystallographic Data Centre via www.ccdc.cam.ac.uk/data_request/cif.

Acknowledgements

This work was supported by a grant from the European Community under the FP6—Marie Curie Host Fellowships for Early Stage Research Training (EST) "CHEMTRONICS" contract number MEST-CT-2005-020513.

[1] a) M. T. Pope, *Heteropoly and Isopoly Oxometalates*, Springer, Berlin, **1983**; b) M. T. Pope, A. Müller, *Angew. Chem.* **1991**, *103*, 56–70; *Angew. Chem. Int. Ed. Engl.* **1991**, *30*, 34–48.
[2] M. T. Pope, *Inorg. Chem.* **1972**, *11*, 1973–1974.
[3] I. A. Weinstock, *Chem. Rev.* **1998**, *98*, 113–170.
[4] M. Sadakane, E. Steckhan, *Chem. Rev.* **1998**, *98*, 219–237.
[5] B. Keita, L. Nadjo, *J. Mol. Catal. A* **2007**, *262*, 190–215.
[6] L. Cheng, J. A. Cox, *Chem. Mater.* **2002**, *14*, 6–8.
[7] a) M. Zynek, M. Serantoni, S. Beloshapkin, E. Dempsey, T. McCormac, *Electroanalysis* **2007**, *19*, 681–689; b) L.-H. Bi, T. McCormac, S. Beloshapkin, E. Dempsey, *Electroanalysis* **2007**, *20*, 38–46.
[8] A. Proust, R. Thouvenot, P. Gouzerh, *Chem. Commun.* **2008**, 1837–1852.
[9] a) D.-L. Long, L. Cronin, *Chem. Eur. J.* **2006**, *12*, 3698–3706; b) D.-L. Long, E. Burkholder, L. Cronin, *Chem. Soc. Rev.* **2007**, *36*, 105–121.
[10] a) S. Liu, D. G. Kurth, D. Volkmer, *Chem. Commun.* **2002**, 976–977; b) S. Liu, D. Volkmer, D. G. Kurth, *Anal. Chem.* **2004**, *76*, 4579–4582.
[11] G. L. Turdean, A. Curulli, I. C. Popescu, C. Rosu, G. Palleschi, *Electroanalysis* **2004**, *16*, 1550–1556.
[12] M. Ammam, B. Keita, L. Nadjo, J. Fransaer, *Sens. Actuators B* **2009**, *142*, 347–354.
[13] T. Yamase, *Chem. Rev.* **1998**, *98*, 307–325.
[14] S. Liu, H. Möhwald, D. Volkmer, D. G. Kurth, *Langmuir* **2006**, *22*, 1949–1951.
[15] a) D. R. Vernon, F. Meng, S. F. Dec, D. L. Williamson, J. A. Turner, A. M. Herring, *J. Power Sources* **2005**, *139*, 141–151; b) R. J. Stanis, M.-C. Kuo, A. J. Rickett, J. A. Turner, A. M. Herring, *Electrochim. Acta* **2008**, *53*, 8277–8286.
[16] a) M. Lu, B. Xie, J. Kang, F.-C. Chen, Y. Yang, Z. Peng, *Chem. Mater.* **2005**, *17*, 402–408; b) B. Xu, M. Lu, J. Kang, D. Wang, J. Brown, Z. Peng, *Chem. Mater.* **2005**, *17*, 2841–2851.
[17] A. K. Cuentas-Gallegos, M. Lirá-Cantu, N. Casañ-Pastor, P. Gómez-Romero, *Adv. Funct. Mater.* **2005**, *15*, 1125–1133.
[18] a) A. M. Douvas, E. Makarona, N. Glezos, P. Argitis, J. A. Mielczarski, E. Mielczarski, *ACS NANO* **2008**, *2*, 733–742; b) E. Kapetanakis, A. M. Douvas, D. Velessiotis, E. Makarona, P. Argitis, N. Glezos, *Org. Electron.* **2009**, *10*, 711–718.
[19] C. Li, W. Fan, B. Lei, D. Zhang, S. Han, T. Tang, X. Liu, Z. Liu, S. Asano, M. Meyyapan, J. Han, C. Zhou, *Appl. Phys. Lett.* **2004**, *84*, 1949–1951.
[20] Q. Li, S. Surthi, G. Mathur, S. Gowda, Q. Zhao, T. A. Sorenson, R. C. Tenent, K. Muthukumaran, J. S. Lindsey, V. Misra, *Appl. Phys. Lett.* **2004**, *85*, 1829–1831.
[21] G. Bidan, E. Jalaguier, PCT Int. Appl., WO 2007015010A1 20070208, **2007**.
[22] a) N. Glezos, D. Velessiotis, G. Chaidogiannos, P. Argitis, D. Tsamakis, X. Zianni, *Synth. Met.* **2003**, *138*, 267–269; b) G. Chaidogiannos, D. Velessiotis, P. Argitis, P. Koutsolelos, C. D. Diakoumakos, D. Tsamakis, N. Glezos, *Microelectron. Eng.* **2004**, *73–74*, 746–751; c) D. Velessiotis, N. Glezos, V. Ioannou-Sougleridis, *J. Appl. Phys.* **2005**, *98*, 084503; d) N. Glezos, A. M. Douvas, P. Argitis, F. Saurenbach, J. Chrost, C. Livitsanos, *Microelectron. Eng.* **2006**, *83*, 1757–1760; e) E. Makarona, E. Kapetanakis, D. M. Velessiotis, A. Douvas, P. Argitis, P. Normand, T. Gotszalk, M. Woszczyna, N. Glezos, *Microelectron. Eng.* **2008**, *85*, 1399–1402.
[23] a) T. He, J. He, M. Lu, B. Chen, H. Pang, W. F. Reus, W. M. Nolte, D. P. Nackashi, P. D. Franzon, J. M. Tour, *J. Am. Chem. Soc.* **2006**, *128*, 14537–14541; b) T. He, S. Ding, N. Peor, M. Lu, D. A. Corley, Y. Gao, S. Itzchaik, J. M. Tour, *J. Am. Chem. Soc.* **2008**, *130*, 1699–1710.
[24] W. G. Klemperer, C. G. Wall, *Chem. Rev.* **1998**, *98*, 297–306.
[25] B. Keita, A. Belhouari, R. Contant, L. Nadjo, *C. R. Acad. Sci. Paris* **1998**, *1*, 333–342.
[26] a) B. Keita, D. Bouaziz, L. Nadjo, *J. Electroanal. Chem.* **1988**, *255*, 307–313; b) B. Keita, D. Bouaziz, L. Nadjo, A. Deronzier, *J. Electroanal. Chem.* **1990**, *279*, 187–203.
[27] a) G. Bidan, E. M. Genies, M. Lapkowski, *J. Chem. Soc. Chem. Commun.* **1988**, 533–535; b) G. Bidan, E. M. Genies, M. Lapkowski, *J. Electroanal. Chem. Interfacial Electrochem.* **1988**, *251*, 297–306.
[28] M. Carraro, M. Gardan, G. Scorrano, E. Fontananova, M. Bonchio, *Chem. Commun.* **2006**, 4533–4535.
[29] a) S. J. Dong, W. Jin, *J. Electroanal. Chem.* **1993**, *354*, 87–97; b) S. J. Dong, M. J. Liu, *J. Electroanal. Chem.* **1994**, *372*, 95–100.
[30] a) P. Judeinstein, *Chem. Mater.* **1992**, *4*, 4–7; b) P. Judeinstein, H. Schmidt, *J. Sol-Gel Sci. Technol.* **1994**, *3*, 189–197.
[31] D. G. Kurth, *Sci. Technol. Adv. Mater.* **2008**, *9*, 014103.
[32] a) C. R. Mayer, V. Cabuil, T. Lalot, R. Thouvenot, *Angew. Chem.* **1999**, *111*, 3878–3881; *Angew. Chem. Int. Ed.* **1999**, *38*, 3672–3675; b) C. R. Mayer, R. Thouvenot, T. Lalot, *Chem. Mater.* **2000**, *12*, 257–260; c) C. R. Mayer, R. Thouvenot, T. Lalot, *Macromolecules* **2000**, *33*, 4433–4437.
[33] R. C. Schroden, C. F. Blanford, B. J. Melde, B. J. S. Johnson, A. Stein, *Chem. Mater.* **2001**, *13*, 1074–1081.
[34] H. Chen, L. Xie, H. Lu, Y. Yang, *J. Mater. Chem.* **2007**, *17*, 1258–1261.
[35] A. R. Moore, H. Kwen, A. M. Beatty, E. A. Maatta, *Chem. Commun.* **2000**, 1793–1794.
[36] a) Y. Wei, B. Xu, C. L. Barnes, Z. Peng, *J. Am. Chem. Soc.* **2001**, *123*, 4083–4084; b) B. Xu, Y. Wei, C. L. Barnes, Z. Peng, *Angew. Chem.* **2001**, *113*, 2353–2356; *Angew. Chem. Int. Ed.* **2001**, *40*, 2290–2292.
[37] Y. Zhu, L. Wang, J. Hao, P. Yin, J. Zhang, Q. Li, L. Zhu, Y. Wei, *Chem. Eur. J.* **2009**, *15*, 3076–3080.
[38] M. Lu, W. M. Nolte, T. He, D. A. Corley, J. M. Tour, *Chem. Mater.* **2009**, *21*, 442–446.
[39] R. J. Errington, S. S. Petkar, B. R. Horrocks, A. Houlton, L. H. Lie, S. N. Patole, *Angew. Chem.* **2005**, *117*, 1280–1283; *Angew. Chem. Int. Ed.* **2005**, *44*, 1254–1257.
[40] Y.-F. Song, N. McMillan, D.-L. Long, S. Kane, J. Malm, M. O. Riehle, C. P. Pradeep, N. Gadegaard, L. Cronin, *J. Am. Chem. Soc.* **2009**, *131*, 1340–1341.
[41] C. Dablemont, A. Proust, R. Thouvenot, C. Afonso, F. Fournier, J.-C. Tabet, *Dalton Trans.* **2005**, 1831–1841.
[42] a) A. Mazeaud, N. Ammari, F. Robert, R. Thouvenot, *Angew. Chem.* **1996**, *108*, 2089–2091; *Angew. Chem. Int. Ed. Engl.* **1996**, *35*,

1961–1964; b) D. Agustin, C. Coelho, A. Mazeaud, P. Herson, A. Proust, R. Thouvenot, *Z. Anorg. Allg. Chem.* **2004**, *630*, 2049–2053.
[43] G. Sazani, M. T. Pope, *Dalton Trans.* **2004**, 1989–1994.
[44] J. Li, R. Tan, R. Li, X. Wang, E. Li, F. Zhai, S. Zhang, *Inorg. Chem. Commun.* **2007**, *10*, 216–219.
[45] H. Günther, *Angew. Chem.* **1972**, *84*, 907–920; *Angew. Chem. Int. Ed. Engl.* **1972**, *11*, 861–874.
[46] R. Massart, R. Contant, J.-M. Fruchart, J.-P. Ciabrini, M. Fournier, *Inorg. Chem.* **1977**, *16*, 2916–2921.
[47] L. Alloul, N. Ammari, C. R. Mayer, A. Mazeaud, R. Thouvenot, *J. Chim. Phys.* **1998**, *95*, 289–294.
[48] Y. Jeannin, M. Fournier, *Pure Appl. Chem.* **1987**, *59*, 1529–1548; Y. Jeannin, *Chem. Rev.* **1998**, *98*, 51–76.
[49] D. Agustin, J. Dallery, C. Coelho, A. Proust, R. Thouvenot, *J. Organomet. Chem.* **2007**, *692*, 746–754.
[50] S. Bareyt, R. Thouvenot, unpublished results.
[51] P. J. Domaille, *J. Am. Chem. Soc.* **1984**, *106*, 7677–7687.
[52] a) J. Niu, M. Li, J. Wang, *J. Organomet. Chem.* **2003**, *675*, 84–90; b) J. Niu, J. Zhao, J. Wang, M. Li, *J. Mol. Struct.* **2003**, *655*, 243–250.
[53] V. Artero, A. Proust, *Eur. J. Inorg. Chem.* **2000**, 2393–2400.
[54] a) S. Himeno, M. Takamoto, *J. Electroanal. Chem.* **2002**, *528*, 170–174; b) S. Himeno, M. Takamoto, A. Higuchi, M. Maekawa, *Inorg. Chim. Acta* **2003**, *348*, 57–62.
[55] a) H. C. Choi, J. M. Buriak, *Chem. Mater.* **2000**, *12*, 2151–2156; b) E. G. Robins, M. P. Stewart, J. M. Buriak, *Chem. Commun.* **1999**, 2479–2480.
[56] K. Huang, F. Duclairoir, T. Pro, J. Buckley, G. Marchand, E. Martinez, J.-C. Marchon, B. De Salvo, G. Delapierre, F. Vinet, *ChemPhysChem* **2009**, *10*, 963–971.
[57] E. Radkov, R. H. Beer, *Polyhedron* **1995**, *14*, 2139–2143.
[58] H. E. Gottlieb, V. Kotlyar, A. Nudelman, *J. Org. Chem.* **1997**, *62*, 7512–7515.
[59] R. Acerete, C. F. Hammer, L. C. W. Baker, *J. Am. Chem. Soc.* **1979**, *101*, 267–269.
[60] A. J. M. Duisenberg, L. M. J. Kroon-Batenburg, A. M. M. Schreurs, *J. Appl. Crystallogr.* **2003**, *36*, 220–229.
[61] R. H. Blessing, *Acta Crystallogr. Sect. A* **1995**, *51*, 33–38.
[62] SHELXL 97: Program for the crystal structure determination, G. M. Sheldrick, University of Göttingen, Göttingen, **1997**.
[63] Diamond, K. Brandenburg, M. Berndt, Crystal Impact GbR, Bonn, **1999**.

Received: December 4, 2009
Published online: March 26, 2010

